J|A|C|S
ARTICLES
Published on Web 04/05/2003

Nitric Oxide-Releasing Fumed Silica Particles: Synthesis, Characterization, and Biomedical Application

Huiping Zhang,[†] Gail M. Annich,[‡] Judiann Miskulin,[‡] Kelly Stankiewicz,[†] Kathryn Osterholzer,[§] Scott I. Merz,[§] Robert H. Bartlett,[‡] and Mark E. Meyerhoff*,[†]

Contribution from the Department of Chemistry, and Department of Surgery, University of Michigan, Ann Arbor, Michigan 48109, and Michigan Critical Care Consultants, Inc., Ann Arbor, Michigan 48103

Received October 30, 2002; E-mail: mmeyerho@umich.edu

Abstract: The preparation, characterization, and preliminary biomedical application of various nitric oxide (NO)-releasing fumed silica particles (0.2−0.3 μm) are reported. The tiny NO-releasing particles are synthesized by first tethering alkylamines onto the surface of the silica using amine-containing silylation reagents. These amine groups are then converted to corresponding *N*-diazeniumdiolate groups via reaction with $NO_{(g)}$ at high pressure in the presence of methoxide bases (e.g., NaOMe). *N*-Diazeniumdiolate groups were found to form more readily with secondary amino nitrogens than primary amino nitrogens tethered to the silica. Different alkali metal cations of the methoxide bases, however, have little effect on the degree of *N*-diazeniumdiolate formation. The *N*-diazeniumdiolate moieties attached on the silica surface undergo a primarily proton-driven dissociation to NO under physiological conditions, with an "apparent" reaction order somewhat greater than 1 owing to local increases in pH at the surface of the particles as free amine groups are generated. The rates of *N*-diazeniumdiolate dissociation are further related to the parent amine structures and the pH of the soaking buffer. The *N*-diazeniumdiolate groups also undergo slow thermal dissociation to NO, with zero-order dissociation observed at both −15 and 23 °C. It is further shown that the resulting NO-releasing fumed silica particles can be embedded into polymer films to create coatings that are thromboresistant, via the release of NO at fluxes that mimic healthy endothelial cells (EC). For example a polyurethane coating containing 20 wt % of NO-releasing particles prepared with pendant hexane diamine structure (i.e., Sil-2N[6]-N_2O_2Na) is shown to exhibit improved surface thromboresistivity (compared to controls) when used to coat the inner walls of extracorporeal circuits (ECC) employed in a rabbit model for extracorporeal blood circulation.

Introduction

Although a wide variety of polymers are currently employed to prepare various blood-contacting medical devices (e.g., catheters, extracorporeal heart bypass circuits, oxygenators, etc.), the thrombogenic nature of such materials can cause serious complications (e.g., thrombosis, bleeding, etc.) in patients and ultimately functional failure.[1−9] As a result, systemic anticoagulation treatments (e.g., use of heparin) are almost always required clinically in extracorporeal procedures to reduce the formation of fibrin clots. The use of large doses of anticoagulants, however, can also have adverse effects, especially an increased risk of hemorrhage. In addition, even when anticoagulant levels can be managed effectively, thrombocytopenia (platelet consumption) and bleeding can still occur.[3,10]

Numerous approaches aimed at developing more blood compatible materials are currently being investigated in many research laboratories worldwide. They can be generally categorized into methods based on mimicking nonthrombogenic endothelial cells (EC),[3,7,11−14] which line the inner walls of all blood vessels, or approaches that employ chemical surface structures that suppress blood−material interactions (e.g.,

[†] Department of Chemistry, University of Michigan.
[‡] Department of Surgery, University of Michigan.
[§] Michigan Critical Care Consultants, Inc.

(1) Didisheim, P. *Cardiovasc. Pathol.* **1993**, *2*, 1S.
(2) Peppas, N. A.; Langer, R. *Science* **1994**, *263*, 1715.
(3) Annich, G. M.; Meinhardt, J. P.; Mowery, K. A.; Ashton, B. A.; Merz, S. I.; Hirschl, R. B.; Meyerhoff, M. E.; Bartlett, R. H. *Crit. Care Med.* **2000**, *28*, 915.
(4) Ratner, B. D. *J. Biomed. Mater. Res.* **1993**, *27*, 283.
(5) Szycher, M. Medical/Pharmaceutical Markets for Medical Plastics. In *High Performance Biomaterials*; Szycher, M., Ed.; Technomic: Lancaster, 1991; pp 3−40.
(6) Greco, R. S., Ed. *Implantation Biology: The Host Response and Biomedical Devices;* CRC Press: Boca Raton, 1994.
(7) Wise, D. L., Gresser, J. D., Trantolo, D. J., Cattaneo, M. V., Lewandrowski, K. U., Yaszemski, M. J., Eds. *Biomaterials Engineering and Devices: Human Applications;* Humana Press: Totowa, NJ, 2000; Vol. 1.
(8) Tanzawa, H. Biomedical Polymers: Current Status and Overview. In *Biomedical Applications of Polymeric Materials*; Tsuruta, T., Hayashi, T., Kataoka, K., Ishihara, K., Kimura, Y., Eds.; CRC Press: Boca Raton, 1993; pp 1−15.
(9) Van Der Kamp, K. W. H. J. *The Interactions of Blood with Polymeric Materials;* Groningen: Rijksuniversiteit Groningen, 1995.
(10) McCrae, K. R.; Cines, D. B. Drug-Induced Thrombocytopenias. In *Thrombosis and Hemorrhage*, 2nd ed.; Loscalzo, J., Schafer, A. I., Eds.; Williams & Wilkins: Baltimore, 1998; Chapter 29, pp 617−642.
(11) Schoenfisch, M. H.; Mowery, K. A.; Rader, M. V.; Baliga, N.; Wahr, J. A.; Meyerhoff, M. E. *Anal. Chem.* **2000**, *72*, 1119.
(12) Zhang, H.; Annich, G. M.; Miskulin, J.; Osterholzer, K.; Merz, S. I.; Bartlett, R. H.; Meyerhoff, M. E. *Biomaterials* **2002**, *23*, 1485.
(13) Feng, J.; Chaikof, E. L. *Polym. Prepr.* **2000**, *41* (2), 16.
(14) Bamford, C. H.; Middleton, I. P.; Al-Lamee, K. G.; Paprotny, J. J. *Int. J. Artif. Organs* **1992**, *15*, 71.

polymeric surfaces that exhibit decreased protein[15,16] and cell adhesion[17−19]). The approaches that mimic the nonthrombogenic EC appear most promising. Molecules contributing to the nonthrombogenic properties of the EC,[20,21] including nitric oxide (NO) and thrombomodulin, can be incorporated into/on polymer matrixes in such a way that they either are released from the polymers[3,11,12,14] or are present on the polymers' surfaces.[7,13] Indeed, recent research in this laboratory[3,11,12] and elsewhere[22] has demonstrated that polymers that can continuously release low levels of NO greatly reduce the platelet activation and adhesion on the surfaces of various materials in vivo. Nitric oxide is well known as a potent antiplatelet agent, and its continuous release from the surface of EC effectively prevents the activation of platelets on the walls of healthy blood vessels.[21,23−25] The NO-flux from normal and stimulated EC has been estimated to be in the range $(0.5-4.1) \times 10^{-10}$ mol/cm^2·min.[23,26]

Nitric oxide-releasing polymers may be prepared by either doping/dispersing various NO-donors into polymer matrixes[3,11] or covalently bonding NO-donors directly onto polymers.[12,27,28] *N*-Diazeniumdiolates (RR′N-$N_2O_2^-$)[29−35] are typical NO-donors employed to develop NO-releasing polymers, as they spontaneously dissociate into NO and parent amines in aqueous media (e.g., blood). Unlike most other NO-donors,[36,37] they do not require either an enzyme or a cofactor to generate NO. In previous work, hydrophobic polymers doped with a *N*-diazeniumdiolate compound, *N*-methyl-*N*-[6-(*N*-methylammoniohexyl)-amino]diazen-1-ium-1,2-diolate (MAHMA-N_2O_2), were shown to exhibit improved blood compatibility in vivo;[3,11] however, hydrophilic MAHMA-N_2O_2 was subsequently found to leach from polymer matrixes into blood, which could cause a potential toxicity issue since it could be oxidized in blood to a carcinogenic *N*-nitrosamine substance.[27] This toxicity concern, however, can be overcome by anchoring such *N*-diazeniumdiolates onto polymer matrixes including poly(vinyl chloride),[27] silicone rubber,[12] acrylate-based polymers,[28] and other polymers typically used in the biomedical arena.

An alternate strategy for the development of useful NO-releasing polymers is reported in detail herein. In this new approach *N*-diazeniumdiolates are tethered onto the surface of tiny fumed silica particles (amorphous silicon dioxide, 0.2−0.3 μm) that are then embedded within given polymer matrixes. In fact, fumed silica is already commonly employed as a reinforcing filler in many polymers;[38] hence, incorporating NO-releasing silica particles within various polymer matrixes provides a potentially more generic approach to devise a wide range of NO-releasing polymers, compared to methods that involve synthesizing a specific NO-releasing macromolecule. Beyond embedding such small NO-releasing particles within polymer films to create more thromboresistant surfaces, the new NO-releasing materials could also be potentially useful for a number of other applications including within topical creams to enhance wound healing, locally vasodilate blood vessels, etc. In this report, the synthesis and NO-release characteristics of a number of different *N*-diazeniumdiolate-functionalized fumed silica particles are presented. In addition, results from preliminary in vivo blood compatibility testing of polyurethane (PU) films doped with these new NO-releasing particles and coated on the inner walls of tubing used in extracorporeal animal experiments are reported.

Experimental Section

Materials. Fumed silica (Cab-O-Sil EH-5, surface area 380 m^2/g, 2.5 mmol/g surface silanol groups) was a gift from Cabot (Tuscola, IL) and was used without any further pretreatment. The amine-containing silanes, including 3-aminopropyltrimethoxysilane, *N*-methyl-3-aminopropyltrimethoxysilane, *N*-(2-aminoethyl)-3-aminopropyltrimethoxysilane, and *N*-(6-aminohexyl)-3-aminopropyltrimethoxysilane, were obtained from Gelest (Tullytown, PA). Nitric oxide (NO) and argon (Ar) gases were from Cryogenic Gases (Detroit, MI). Sodium methoxide (NaOMe), potassium methoxide (KOMe), lithium methoxide (LiOMe), phosphate buffered saline (PBS, pH 7.4), 2-[*N*-morpholino]-ethanesulfonic acid (MES), *N*-tris[hydroxymethyl]methyl-4-aminobutanesulfonic acid (TABS), and (3-[cyclohexylamino]-1-propanesulfonic acid (CAPS) were purchased from Sigma-Aldrich (Milwaukee, WI). Carbonthane 3575A (a medical grade PU elastomer) was a gift from VIASYS Healthcare (Woburn, MA). Medical grade Tygon PVC tubing (i.d., 0.635 cm), toluene, methanol (MeOH), tetrahydrofuran (THF), and *N*,*N*-dimethylformamide (DMF) were from Fisher Scientific (Pittsburgh, PA). Methanol and DMF were dehydrated over 3 and 4 Å molecular sieves, respectively. Dry THF was obtained from a THF still, where THF was refluxed and distilled over sodium metal and benzophenone. All other reagents were used as received.

Synthesis of NO-Releasing Fumed Silica Particles (Sil-N_2O_2M; Scheme 1). Fumed silica particles (10 g, ca. 25 mmol of surface silanol groups) were suspended in toluene (450 mL) under stirring, and the mixture was refluxed for 5 min. An equimolar amount of amine-containing silane (25 mmol, e.g., 6.96 g of *N*-(6-aminohexyl)-3-aminopropyltrimethoxysilane) in toluene solution (50 mL) was then

(15) Whitesides, G. Biological Surface Science. In *Transactions of the 6th World Biomaterials Congress*; Society of Biomaterials: Minneapolis, 2000; Vol. 1, p 21.
(16) Ishihara, K. *TRIP* **1997**, *5*, 401.
(17) Ryu, G.; Han, D.; Kim, Y.; Min, B. *Am. Soc. Artif. Intern. Organs J.* **1992**, *38*, M644.
(18) Espadas-Torre, C.; Meyerhoff, M. E. *Anal. Chem.* **1995**, *67*, 3108.
(19) Sefton, M. V. *Biomaterials* **1993**, *14*, 1127.
(20) Colman, R. W. *Cardiovasc. Pathol.* **1993**, *2*, 23S.
(21) Makrides, S. C.; Ryan, U. S. Overview of the Endothelium. In *Thrombosis and Hemorrhage*, 2nd ed.; Loscalzo, J., Schafer, A. I., Eds.; Williams & Wilkins: Baltimore, 1998; Chapter 13, pp 295−306.
(22) Smith; D. J.; Chakravarthy, D.; Pulfer, S.; Simmons, M.; Hrabie, J. A.; Citro, M. L.; Saavedra, J. E.; Davies, K. M.; Hutsell, T. C.; Mooradian, D. L.; Hanson, S. R.; Keefer, L. K. *J. Med. Chem.* **1996**, *39*, 1148.
(23) Radomski, M. K.; Palmer, R. M.; Moncada, S. *Biochem. Biophys. Res. Commun.* **1987**, *148*, 1482.
(24) Radomski, M. K.; Salas, E. *Atherosclerosis* **1995**, *118*, S69.
(25) Cheung, P. Y.; Salas, E.; Etches, P. C.; Schulz, R.; Radomski, M. W. *Lancet* **1998**, *351*, 1181.
(26) Vaughn, M. W.; Kuo, L.; Liao, J. C. *Am. J. Physiol.* 274 (*Heart Circ. Physiol.* 43) **1998**, H2163.
(27) Mowery, K. A.; Schoenfisch, M. H.; Saavedra, J. E.; Keefer, L. K.; Meyerhoff, M. E. *Biomaterials* **2000**, *21*, 9.
(28) Parzuchowski, P. G.; Frost, M. C.; Meyerhoff, M. E. *J. Am. Chem. Soc.* **2002**, *124*, 12182.
(29) Hrabie, J. A.; Keefer, L. K. *Chem. Rev.* **2002**, *102*, 1135.
(30) Davies, K. M.; Wink, D. A.; Saavedra, J. E.; Keefer, L. K. *J. Am. Chem. Soc.* **2001**, *123*, 5473.
(31) Hrabie, J. A.; Klose, J. R.; Wink, D. A.; Keefer, L. K. *J. Org. Chem.* **1993**, *58*, 1472.
(32) Maragos, C. M.; Morley, D.; Wink, D. A.; Dunams, T. M.; Saavedra, J. E.; Hoffman, A.; Bove, A. A.; Isaac, L.; Hrabie, J. A.; Keefer, L. K. *J. Med. Chem.* **1991**, *34*, 3242.
(33) Ragsdale, R. O.; Karstetter, B. R.; Dargo, R. S. *Inorg. Chem.* **1965**, *4*, 422.
(34) Drago, R. S. Reactions of Nitrogen(II) Oxide. In *Advances in Chemistry Series* 36; American Chemical Society: Washington, D.C., 1962; pp 143−149.
(35) Drago, R. S.; Ragsdale, R. O.; Eyman, D. P. *J. Am. Chem. Soc.* **1961**, *83*, 4337.
(36) Wang, P. G.; Xian, M.; Tang, X.; Wu, X.; Wen, Z.; Cai, T.; Janczuk, A. J. *Chem. Rev.* **2002**, *102*, 1091.
(37) Hanson, S. R.; Hutsell, T. C.; Keefer, L. K.; Mooradian, D. L.; Smith, D. J. Nitric Oxide Donors: A Continuing Opportunity in Drug Design. In *Nitric Oxide: Biochemistry, Molecular Biology, and Therapeutic Implications*; Ignarro, L., Murad, F., Eds.; Academic Press: San Diego, CA, 1995; pp 383−397.
(38) *Cab-O-Sil Untreated Fumed Silica Properties and Functions*, A *Cabot Technical Brochure*, 1996.

Scheme 1. Synthesis Route to Sil-N_2O_2M Particles[a]

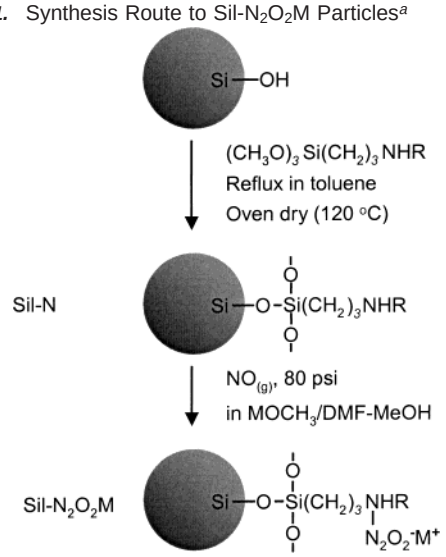

[a] R = Table 1, M = Na^+, K^+, and Li^+.

Table 1. Different Amines Linked to Fumed Silica Particles in Accordance with Scheme 1

R group	abbreviation of pendant amine species
H	1N-H
CH_3	1N-C1
$(CH_2)_2NH_2$	2N[2]
$(CH_2)_6NH_2$	2N[6]

added to the above suspension. The mixture was further refluxed with stirring overnight. After cooling to ambient temperature, the mixture was centrifuged at 3000 rpm for 5 min (Centrifuge 5810 R, Eppendorf). The silica pellets were resuspended in toluene and centrifuged again. This toluene-rinse step was repeated two more times in order to remove unattached silanes. The amine-functionalized silica particles (Sil-N, see Table 1) were then oven-dried at 120 °C overnight.

The resulting Sil-N particles were ground using a mini-bead-beater (Wig-L-Bug, Aldrich). The ground particles (1.5 g, 1.5−2.3 mmol of various surface appended amines) were then suspended in one of the following alkaline solutions in a 500 mL Parr bottle: 0.02−0.44 M NaOMe or KOMe in a mixture of dry DMF−MeOH (9:1) (150 mL, 3 to 66 mmol NaOMe or KOMe) or 0.02−0.44 M LiOMe in a mixture of dry DMF−MeOH (1:1) (150 mL, 3−66 mmol LiOMe). The Parr bottle was then connected to the NO-reactor (modified from the Parr hydrogenation system) and charged/discharged six times with argon to remove any oxygen in the suspension. The reaction bottle was then charged with $NO_{(g)}$ to 80 psi and closed. After 21 h, the reaction bottle was discharged with $NO_{(g)}$ and purged with $Ar_{(g)}$ using the same purging procedure described earlier to remove unreacted $NO_{(g)}$. The slurry of the *N*-diazeniumdiolated silica particles was centrifuged at 4000 rpm for 10 min. The Sil-N_2O_2M pellets were then rinsed with the following solutions by resuspension and centrifugation: 0.02 M MOH (the same alkali metal cation as used in the NO-addition reaction) in a methanol−water (2:1) mixture (twice); 0.02 M MOMe in methanol (once); and THF (three times). The Sil-N_2O_2M particles were then vacuum-dried overnight and stored at −20 °C.

Characterization of the Sil-N and Sil-N_2O_2M Particles. Elemental (CHN) analysis was carried out on a Perkin-Elmer 2400 Series II analyzer to determine the content of amines attached to the surface of fumed silica particles (see Supporting Information file for details). The UV−vis spectra of various Sil-N_2O_2M particles dissolved in the corresponding 1 M MOH aqueous solution at a concentration of 0.2 mg/mL were recorded on a Beckman DU 640B spectrophotometer. It was found that complete dissolution of the particles occurred under such basic conditions. The *N*-diazeniumdiolate content (C_d, mmol/g) of a Sil-N_2O_2M particle was determined by measuring the total amount of NO-release from the particles using a Sievers NOA 280i chemiluminescence NO-analyzer (nitrogen as a carrier gas) (see Supporting Information file for details of calculation method).

Kinetic Studies of the Dissociation of Sil-N_2O_2M Particles. Chemiluminescence was used to study the kinetics of the dissociation of various Sil-N_2O_2M particles in PBS buffer at 37 °C (physiological conditions). Four NO-release/*N*-diazeniumdiolate dissociation plots were derived for each chemiluminescence measurement: (1) chemiluminescence response in ppb NO vs time; (2) total amount of NO-release vs time; (3) ln v vs lnC_d, where v is the dissociation rate of the *N*-diazeniumdiolate ($-dC_d/dt$); and (4) C_d vs time.

The "apparent" half-life ($t_{1/2}$) of given Sil-N_2O_2M particles was determined from the plot 2, at the time point when half the total amount of NO was released. The "apparent" reaction order (n) of the *N*-diazeniumdiolate dissociation was determined from the slope of plot 3, while the intercept of plot 3 is ln k, where k is the "apparent" dissociation rate constant. If a zero-order dissociation was determined from plot 3, plot 4 was subsequently employed to further confirm that the reaction order is zero.

In addition to studying rates of dissociation under physiological conditions, NO-release from the Sil-2N[6]-N_2O_2Na particles at pH's other than 7.4 were also examined to investigate the influence of pH on the *N*-diazeniumdiolate dissociation rate. The buffers used for these pH studies included MES (pH 6.0, 0.2 M), TABS (pH 9.0, 0.2 M), and CAPS (pH 11.0, 0.2 M). Furthermore, the thermal dissociation of dry Sil-2N[6]-N_2O_2Na particles at different temperatures (−15, 23, and 80 °C) was also investigated. Due to slow dissociation rates at −15 and 23 °C, the "apparent" $t_{1/2}$ values under these conditions were determined from the extrapolation of plot 4 instead of directly from plot 2.

Preparation of PU/Sil-2N[6]-N_2O_2Na Coating on the Inner Wall of PVC Tubing. For extracorporeal animal experiments, medical grade Tygon PVC tubings were coated with PU/Sil-2N[6]-N_2O_2Na to make extracorporeal (ECC) circuits. All coatings were prepared by Michigan Critical Care Consultants, Inc (Ann Arbor, MI). The coating (overall thickness ca. 210 μm) contained four layers in the following order from the tubing inner wall to innermost blood-contacting surface: (1) a PU bottom coat; (2) a 80%/20% PU/Sil-2N[6]-N_2O_2Na layer (active layer); (3) a PU topcoat; and (4) a PVC topcoat employed to achieve a blood-contacting surface identical to that of bare PVC tubing. The corresponding cocktail solutions for each layer were as follows: (1) PU (2.0 g) dissolved in THF (20 mL); (2) a PU/THF solution (3.9 g PU in 20 mL of THF) mixed with a Sil-2N[6]-N_2O_2Na/THF suspension (0.98 g of particles dispersed in 31 mL of THF); (3) PU (2.7 g) in THF (20 mL); and (4) Tygon PVC tubing (2.0 g) dissolved in THF (30 mL). Approximately 1 m lengths of PVC tubing were coated by adding each of the above cocktail solutions sequentially and allowing the bolus of solution to flow through the entire length of the tubing. The excess solution was discarded, and the tubing was extended horizontally and rotated slowly to ensure an even coating during curing. Nitrogen gas was passed through the tubing to accelerate the drying process and to minimize oxygen and water vapor exposure for the circuits. Typical drying times were 24 h.

For control circuits, the original untreated fumed silica particles were used instead of the Sil-2N[6]-N_2O_2Na particles to formulate the exact same coatings. The control circuits were handled in the same manner as the PU/Sil-2N[6]-N_2O_2Na circuits, except that compressed air was used for drying the control circuits.

Rabbit Extracorporeal Circulation (ECC) Experiments. All animal testing was carried out in the ECMO (extracorporeal membrane oxygenation) lab at the Medical Center of the University of Michigan using a rabbit ECC model.[3] Briefly, the coated PVC tubings were connected to a rabbit through two cannulas for venovenous circulation (jugular veins) via a roller pump, and the blood was circulated through

Table 2. Results of Amine-Functionalization of Fumed Silica Particles (Sil-N)[a]

parent amine	amine content[a] (mmol/g)	coupling efficiency (%)
1N-H	1.52	71
1N-C1	1.31	59
2N[2]	1.47	70
2N[6]	1.00	49

[a] Amine content is the content of diamine if the pendant amine is a diamine, or a content of monoamine if the pendant amine is a monoamine.

the tubing for 4 h. Platelet counts were obtained at the beginning and each hour thereafter using a Beckman-Coulter model Z_1 particle counter. At the end of each experiment, the tubing was removed, rinsed with normal saline (0.9 wt % saline), fixed with a 2 wt % aqueous glutaraldehyde solution, and dehydrated sequentially with 30, 50, 70, 90, 95, and 100% (v/v) ethanol and hexamethyldisilazane.

A scanning electron microscope (Hitachi S-3200N) was used to examine platelet adhesion/activation on the coating surface. One centimeter segments of each of the circuits were selected for examination at the following locations: (1) immediately distal to the drainage cannula; (2) region within the roller pump; (3) exit from the roller pump; and (4) immediately distal to the infusion cannula. These tubing pieces were cut in half, sputter-coated with gold, and examined on their inner surfaces for surface platelet adhesion and activation using the SEM operated at 20 kV.

Results and Discussion

Amine-Functionalized Fumed Silica (Sil-N) Particles. The coupling reaction (see Scheme 1) of various amine-containing trimethoxysilanes (Table 1) with fumed silica is well reported in the literature.[38−41] Although there is still debate on whether the Si−O−Si bond between silica surface and silylating agents is formed before or after oven-drying,[42−45] there is general agreement that the silylating agents are covalently attached to the silica surface after the oven-drying step. On the basis of results from CHN analysis, 50−70 mol % of starting silanes were coupled onto the fumed silica particles employed in this work (see Table 2).

***N*-Diazeniumdiolate Formation on Surface of Sil-N Particles.** The amine groups on the surface of Sil-N particles were then reacted with $NO_{(g)}$ to form corresponding *N*-diazeniumdiolate groups (see Scheme 1).

In Neat Solvent. In initial studies of the NO-addition reaction, Sil-2N[6] particles were suspended in a neat solvent (e.g., acetonitrile) and reacted with $NO_{(g)}$ at high pressure (80 psi). This is the typical synthetic route used to form free *N*-diazeniumdiolate compounds well cited in the literature.[31,32,34,35] The *N*-diazeniumdiolate species formed includes a *N*-diazeniumdiolate anion and an ammonium countercation, where the ammonium countercation is from either an adjacent amine on the same structure (e.g., for diamines) or a second molecule containing an amine site (e.g., for monoamines).[31,32,34,35]

Scheme 2. Modified Mechanism of *N*-Diazeniumdiolate Formation/Dissociation from the One Proposed by R. S. Drago[33−35]

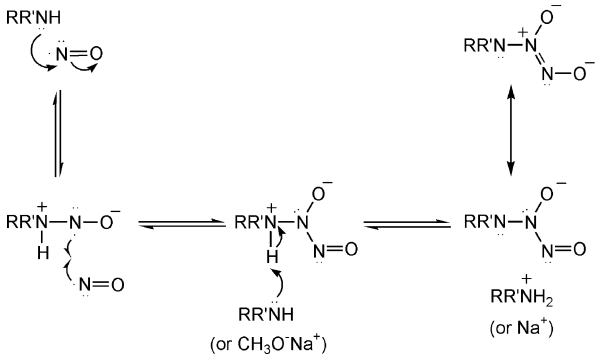

Table 3. Effect of NaOMe Concentration on the NO-Addition for Sil-2N[6] Particles

NaOMe conc (M)	content of remaining diamine (mmol/g)[a]	*N*-diazeniumdiolate content (C_d, mmol/g)	NO-addition efficiency
0.02	0.86	0.28	33%
0.10	0.57	0.20	35%
0.44	0.42	0.13	31%

[a] Original diamine content is 1.0 mmol/g.

The NO-addition efficiency for this direct reaction, however, was found to be very low (12% when acetonitrile was used as the solvent) for the Sil-2N[6] particles, compared to a typical yield of 30−90% for various free amines.[31] A major reason for such a low efficiency of the direct NO-addition reaction with the diamine structure appended to the fumed silica could be related to the equilibrium constant for *N*-diazeniumdiolate formation under the given experimental conditions. In the case of freely soluble amines, the *N*-diazeniumdiolate products always precipitate out of the reaction solution,[31,32,34,35] which drives the reaction equilibrium toward the formation of the product and, in turn, provides a relatively high yield. In the case of Sil-2N[6] particles, however, such a driving force is minimal, as no obvious phase separation occurs on the silica surface during the reaction.

Use of Sodium Methoxide Base. To increase the NO-addition efficiency, various bases were used to shift the reaction equilibrium toward diazeniumdiolate product formation. It was found that when sodium methoxide (NaOMe) was used, the reaction efficiency was increased more than 2-fold (for example, from 12% to 33% when a 0.02 M NaOMe solution was employed). Such an increase is also clearly evident in the UV spectra of the dissolved particles, where the *N*-diazeniumdiolate absorbance was dramatically increased after use of NaOMe (data not shown). Indeed, as suggested in the mechanism of *N*-diazeniumdiolate formation/dissociation initially proposed by Drago,[33−35] a strong base like NaOMe would favor the deprotonation of the amino nitrogen (the third step), which shifts the equilibrium toward *N*-diazeniumdiolate formation (Scheme 2).

Unfortunately, the use of NaOMe was also found to cleave some of the covalently linked amino groups by breaking Si−O−Si bonds, which are known to be labile to base. As shown in Table 3, the more concentrated the base used, the lower the total amino groups found bonded to the silica surface, as determined by CHN analysis. At the same time, the NO-addition efficiency was not affected by the base concentration (see Table 3). Therefore, a low base concentration (e.g., 0.02 M) was

(39) Blitz, J. P.; Shreedhara Murthy, R. S. S.; Leyden, D. E. *J. Colloid Interface Sci.* **1988**, *126*, 387.
(40) Engelhardt, H.; Orth, P. *J. Liq. Chromatgr.* **1987**, *10*, 1999.
(41) Arkles, B. *Chemtech.* **1977**, *7*, 766.
(42) Waddell, T. G.; Leyden, D. E.; DeBello, M. T. *J. Am. Chem. Soc.* **1981**, *103*, 5303.
(43) Van Der Voort, P.; Vansant, E. F. *J. Liq. Chrom. Relat. Technol.* **1996**, *19*, 2723.
(44) Vandenberg, E. T.; Bertilsson, L.; Liedberg, B.; Uvdal, K.; Erlandsson, R.; Elwing, H.; Lundstrom, I. *J. Colloid Interface Sci.* **1991**, *147*, 103.
(45) Plueddemann, E. P. Chemistry of Silane Coupling Agents. In *Silane Coupling Agents*, 2nd ed.; Plueddemann, E. P., Ed.; Plenum Press: New York, 1991; pp 31−54.

Table 4. Average *N*-Diazeniumdiolate Content (C_d), NO-Addition Efficiency, Nitrite Content, and Percentage of *N*-Diazeniumdiolate Group (P_{diaz}) of Various Sil-N_2O_2Na Particles with Different Amine Structures (N = 5 for Sil-2N[6]-N_2O_2Na Particles; N = 2 Measurements for Other Sil-N_2O_2Na Particles)

parent amine	content of remaining amine (mmol/g)	C_d (mmol/g)	NO-addition efficiency (%)	nitrite content (mmol/g)	P_{diaz} (%)
1N−H	1.28	0.038	3	0.029	57
1N−C1	1.10	0.29	26	0.13	69
2N[2]	1.23	0.29	24	0.12	71
2N[6]	0.86	0.28 ± 0.03	33 ± 3	0.10 ± 0.03	74

employed in this work to minimize the cleavage of pendant amino groups and to achieve a reasonable yield of *N*-diazeniumdiolated Sil-N particles.

It should be noted that the amines cleaved by the added base can also react with $NO_{(g)}$ to form corresponding free *N*-diazeniumdiolated compounds. These byproducts, if not removed, would result in a positive error for the measurement of the amount of *N*-diazeniumdiolate formed on the silica surface. Therefore, considerable effort was made to optimize the workup procedure (see Experimental Section) to avoid this problem. It was found that these byproducts could be washed away from the silica particles using a solution of 0.02 M hydroxide in a methanol−water (2:1) mixture. The methanol−water (2:1) mixture can dissolve the byproducts, while the base minimizes the *N*-diazeniumdiolate dissociation. In addition, a low concentration (0.02 M) of hydroxide was necessary to minimize the possible cleavage of Si−O−Si bonds as discussed above.

Side Product: Nitrite Species. In addition to *N*-diazeniumdiolate species, a given amount of nitrite species was also found to be released initially into a surrounding PBS solution from Sil-2N[6]-N_2O_2Na particles, as determined using the Griess assay.[46] It should be noted that such nitrite measurements were conducted only after all NO was released (and purged with nitrogen) from sample solutions, as NO could eventually be oxidized to nitrite to cause interference. The initial nitrite salt is likely formed either from the reaction of the amine with NO_x (e.g., N_2O_3) and moisture during the $NO_{(g)}$-addition reaction, since small amounts of NO_x gases are always present in a compressed $NO_{(g)}$-tank,[47] or from the decomposition of *N*-diazeniumdiolate by ambient oxygen and moisture during the workup (see possible reactions schemes for nitrite salt formation in Supporting Information file, Scheme 1S).

However, the *N*-diazeniumdiolate species are still the major product from the NO-addition, with ca. 74% of the total reacted amine groups present as *N*-diazeniumdiolates for the Sil-2N-[6]-N_2O_2Na particles (see Table 4). The total N-increase (0.66 mmol/g) due to the formation of *N*-diazeniumdiolate and nitrite, calculated as the sum of *N*-diazeniumdiolate content (C_d) multiplied by 2, plus the nitrite content, matches well with the CHN analysis data (0.72 mmol/g), given the instrumental error of 0.07 mmol/g for the N analysis (calculated from the instrumental error of 0.1 wt % and the atomic mass of 14 for N).

Effect of Amine Structure. For the two monoamines anchored to silica surfaces, 1N-H (a primary amine) and 1N-C1 (a secondary amine) (see Table 1), the corresponding *N*-diazeniumdiolate of the former has a λ_{max} of 252 nm, while the *N*-diazeniumdiolate of the latter has a λ_{max} of 246 nm (see Table 5). For the two diamines examined, 2N[2] and 2N[6] (see Table 1), both have primary and secondary amino nitrogens. After NO-addition, the *N*-diazeniumdiolate group was found to be predominantly attached to the secondary amino nitrogen in both cases, as the λ_{max} was found to be 246 nm (Table 5). This result indicates that the secondary amine sites appended to the silica surfaces are more favorable for reaction with $NO_{(g)}$ than the primary amine sites. This observation is consistent with previous results reporting the exclusive NO-addition with the secondary amino nitrogen of some triamines (e.g., diethylenetriamine).[31] Indeed, it is expected that a stronger nucleophile (i.e., secondary amine) exhibits a higher reactivity toward electrophilic NO, as also suggested by the mechanism for the *N*-diazeniumdiolate formation (Scheme 2), where the first step is the nucleophilic attack of NO by the amine. In fact, due to this preference for secondary amines, the NO-addition efficiencies of secondary amines linked to fumed silica particles (ca. 30%) were found to be much higher than that of the primary amine (3%), as shown in Table 4.

Table 5. *N*-Diazeniumdiolate Content (C_d) and Optical Properties (λ_{Max} and ϵ_{Max}) of Various Sil-N_2O_2M Particles with Different Parent Amine Structures and Different Countercations

	C_d (mmol/g)			ϵ_{max} ($mM^{-1}\cdot cm^{-1}$)			
parent amine	Na^+	K^+	Li^+	Na^+	K^+	Li^+	λ_{max} (nm)
1N-H	0.04	0.03	0.005	39	47	46	252
1N-C1	0.29	0.18	0.30	11.1	11.6	10.3	246
2N[2]	0.29	0.18	0.32	13.1	13.5	11.8	246
2N[6]	0.28	0.30	0.31	12.6	12.8	13.8	246

The molar absorptivities (ϵ_{max}, determined using Beer's law) between *N*-diazeniumdiolated primary amines and secondary amines were also found to be quite different. The former (ca. 40 $mM^{-1}\cdot cm^{-1}$) is much larger than that found for the diamine species (11−13 $mM^{-1}\cdot cm^{-1}$), as shown in Table 5. Even though the specific mechanism is still not clear, the extra hydrogen attached to the primary amino nitrogen and/or the decreased basicity of the secondary amine site appears to be the cause for this ϵ_{max} difference.

For three different secondary amine structures examined (i.e., 1N−C1, 2N[2], and 2N[6]), considerable similarities were found in terms of NO-addition efficiency (Table 4) and optical properties (Table 5), due to the fact that the NO-addition occurs preferentially on secondary amino nitrogens, and the *N*-diazeniumdiolate products formed are thus quite similar.

Effect of Countercations. As the *N*-diazeniumdiolate anion has a pocket-like structure similar to a bidentate ligand such as acetylacetonate,[33,48] with a distance between the centers of two terminal oxygens of ca. 2.6 Å [calculated from the data in ref

(46) Schmidt, H. H. H. W.; Kelm, M. Determination of Nitrite and Nitrate by the Griess Reaction. In *Methods in Nitric Oxide Research*; Feelisch, M., Stamler, J. S., Eds.; John Wiley & Sons: West Sussex, 1996; pp 491−497.

(47) Bonner, F. T.; Stedman, G. The Chemistry of Nitric Oxide and Redox-Related Species. In *Methods in Nitric Oxide Research*; Feelisch, M., Stamler, J. S., Eds.; John Wiley & Sons: West Sussex, 1996; pp 3−18.

48], the *N*-diazeniumdiolate moiety may have a chelating interaction with cations. If this is true, different size and/or type of cations may affect the degree of *N*-diazeniumdiolate formation and stability. To examine this possibility, a series of alkali metal cations with different sizes, diameter of 1.2, 1.9, and 2.7 Å for Na^+, Li^+, and K^+, respectively, were employed during the NO-addition reaction. As indicated in Table 5, the different countercations yielded similar NO-addition efficiencies and optical properties. This result is probably due to the weak tendency for alkali metal cations to complex with chelating reagents in general, with only a few exceptions, such as their interaction with certain crown ethers and calixarenes.[49] Therefore, there is likely only a nonspecific ionic interaction between the countercation and the pendant *N*-diazeniumdiolate anion.

***N*-Diazeniumdiolate Dissociation of the Sil-N_2O_2Na Particles.** *N*-Diazeniumdiolate compounds undergo both proton-driven[30,32] and thermal dissociations.[33,34] Both mechanisms yield 2 mol of NO per mole of *N*-diazeniumdiolate.[30,33] The former was reported to be a pseudo-first-order reaction with respect to the *N*-diazeniumdiolate, where the first-order rate constant (k) changes with proton activity in buffer.[30] The correlation between k and buffer pH depends on the parent amine structure. In general, k decreases as the pH increases.[30] For thermal dissociation, however, the kinetics have not been investigated to date. Chemiluminescence was used herein to study the kinetics of both the proton-driven and thermal dissociation of the Sil-2N[6]-N_2O_2Na particles. Similar kinetic studies were also carried out with the three other structures listed in Table 1.

Dissociation Kinetics of Sil-2N[6]-N_2O_2Na under Physiological Conditions. Two types of NO-release plots, plots 1 and 2 (see Experimental Section), of the Sil-2N[6]-N_2O_2Na particles are shown in Figure 1. It was found that the dry Sil-2N[6]-N_2O_2Na particles spontaneously released a low level of NO at 37 °C (Figure 1a), indicating the existence of thermal dissociation. When PBS buffer was added to the Sil-2N[6]-N_2O_2-Na particles, there was a burst of NO-release, suggesting that protons are the major driving force for *N*-diazeniumdiolate dissociation under the physiological conditions (i.e., in PBS buffer, pH 7.4, at 37 °C). The NO-release contributed from the thermal dissociation can, therefore, be neglected due to such a large difference in NO release rates.

The "apparent" half-life ($t_{1/2}$) of the Sil-2N[6]-N_2O_2Na particles under physiological conditions was found to be 43 min (Figure 1b), longer than the $t_{1/2}$ (2.8 min) of the solution phase analogue *N*-diazeniumdiolate compound, MAHAMA-N_2O_2, which has a structure very similar to the *N*-diazeniumdiolate moiety pendant to the surface of the Sil-2N[6]-N_2O_2Na particles. Apparently, the surface of the Sil-2N[6]-N_2O_2Na particles helps to stabilize the *N*-diazeniumdiolate groups anchored on the surface (see below).

The "apparent" reaction orders (n) of the Sil-2N[6]-N_2O_2Na particles under physiological conditions were determined from the $\ln v - \ln C_d$ plot (Figure 2). As illustrated in Figure 2, the "apparent" n toward *N*-diazeniumdiolate was found to be 1.69 on the silica surface, instead of 1, which was reported in the literature for *N*-diazeniumdiolate dissociation in aqueous media.[30,32] Even though there is considerable deviation from the linear plot during the initial dissociation course (Figure 2), these initial data points may not be representative of the overall dissociation reaction, as there may be some interfering factors, such as the initial wetting of silica particles by the buffer solution, occurring at the beginning of the experiment. Indeed, the slope of 1.69 was obtained on the basis of all data points, which clearly indicates that these few initial data points do not contribute significantly to the overall slope determination.

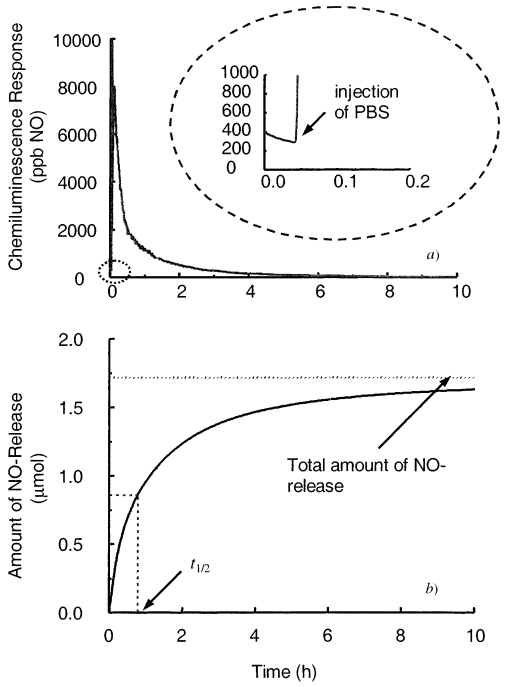

Figure 1. Two types of NO-release profiles of the Sil-2N[6]-N_2O_2Na particles (3.02 mg) in PBS (pH = 7.4, 15 mL) at 37 °C: (a) chemiluminescence response (ppb NO) vs time and (b) amount of NO-release vs time.

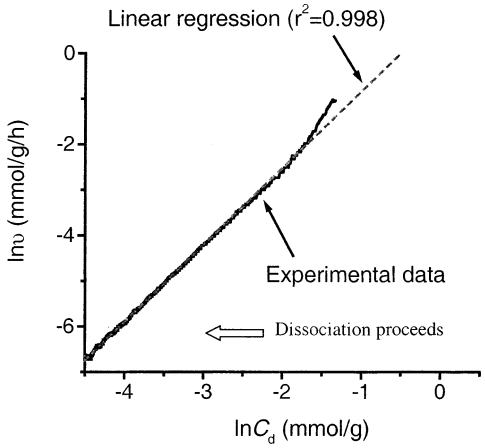

Figure 2. ln v vs ln Cd plot for the dissociation of the Sil-2N[6]-N_2O_2Na particles under physiological conditions, with a linear slope of 1.69.

Such an increase of reaction order is likely due to a local pH increase on the silica surface as the *N*-diazeniumdiolates dissociates and more and more secondary amines are generated on the silica surface, which increases the local pH at the silica surface. Indeed, it is not uncommon that the pH of a surface is different from the pH in the bulk solution. It was reported that certain biological surfaces (e.g., colonic epithelium) maintains a surface pH that is different from the pH in luminal buffer solution (i.e., bulk pH).[50] It has also been reported in the

(48) Keefer, L. K.; Flippen-Anderson, J. L.; George, C.; Shanklin, A. P.; Dunamas, T. A.; Christodoulou, D.; Saavedra, J. E.; Sagan, E. S.; Bohle, D. S. *Nitric Oxide Biol. Chem.* **2001**, *5*, 377.
(49) Wang, J. *Analytical Electrochemistry*; VCH Press: New York, 1994; p 120.

Table 6. Effect of Buffer pH on the Dissociation Kinetics of the Sil-2N[6]-N_2O_2 Na Particle in Various Buffers at 37 °C

pH in buffer	"apparent" $t_{1/2}$ (min)	*n*
6.0	15	1.72
7.4	43	1.69
9.0	119	1.29
11.0	5.60×10^3	0[a]

[a] The apparent *n* at pH 11.0 changes as dissociation proceeds and eventually goes to 0.

literature that the adsorption of certain chemicals on given surfaces, e.g., a cationic surfactant on a carbon electrode surface,[51] or some detergents on skin surfaces,[52] or a fatty acid on an epithelial surface,[50] can change the surface pH. Such a surface pH change due to the generation of amines is likely to cause the apparent reaction order to rise above 1. Indeed, the *N*-diazeniumdiolate moieties on the silica surface probably still undergo first-order dissociation; however, as dissociation proceeds, the local pH on the surface increases, causing the first-order dissociation rate constant to decrease. As a result, the slope of the ln υ vs ln C_d plot appears larger than 1. In addition to yielding a larger "apparent" reaction order, the local pH increase can also result in a longer $t_{1/2}$ value due to a continuous decrease of the first-order dissociation rate constant.

Effect of Buffer pH on Decomposition Rate. As the buffer pH increases, the apparent $t_{1/2}$ of Sil-2N[6]-N_2O_2Na particles was found to increase (see Table 6), as expected for a proton-driven dissociation. At pH 6.0 and 9.0, the kinetic data (i.e., linear ln υ−ln C_d plots, data not shown) are similar to that for pH 7.4, with apparent reaction orders found to be 1.72 and 1.29, respectively. At pH 11.0, however, the ln υ−ln C_d plot (Figure 3) was found to be nonlinear. As shown in Figure 3a, the apparent reaction order continuously changes and tends to go toward zero as dissociation proceeds. After 5 h of dissociation, a linear $C_d - t$ plot ($r^2 = 0.999$) was achieved (see Figure 3b), which is the characteristics of a zero-order reaction. This zero-order dissociation is in fact only observed for a thermal dissociation (see below). Apparently, the thermal dissociation pathway tends to dominate at pH 11.0, where proton activity in the buffer is very low, and hence the proton-driven dissociation becomes much slower than thermal dissociation.

Thermal Dissociation Kinetics of Sil-2N[6]-N_2O_2Na. The apparent half-lives for dry Sil-2N[6]-N_2O_2Na particles at different temperatures are listed in Table 7. As anticipated, the stability of the Sil-2N[6]-N_2O_2Na particle decreases as temperature increases. The particles are relatively stable at −15 °C, with a half-life of ca. 70 days. At −15 °C, the dry Sil-2N[6]-N_2O_2Na particles were found to undergo zero-order thermal dissociation, as demonstrated via both ln υ−ln C_d and C_d−t plots (see Figure 4). The dissociation rate remains constant and does not vary with a change of *N*-diazeniumdiolate content on the silica surface. At ambient temperature (23 °C), the dissociation kinetics of dry Sil-2N[6]-N_2O_2Na particles were found to be similar to that observed for the same particles in a pH 11 buffer (data not shown).

At 80 °C, the dissociation kinetics were found to be more complex (data not shown). The apparent reaction order was found to change throughout the entire dissociation course, and no zero-order dissociation was observed. Since the thermal dissociation mechanism for *N*-diazeniumdiolates is not yet known, it is difficult to assess, at present, the reason for this change. Clearly, for practical use of these NO-releasing particles, they should be stored at low temperatures, preferably at −15 °C or lower, to avoid significant thermal loss of *N*-diazeniumdiolate moieties.

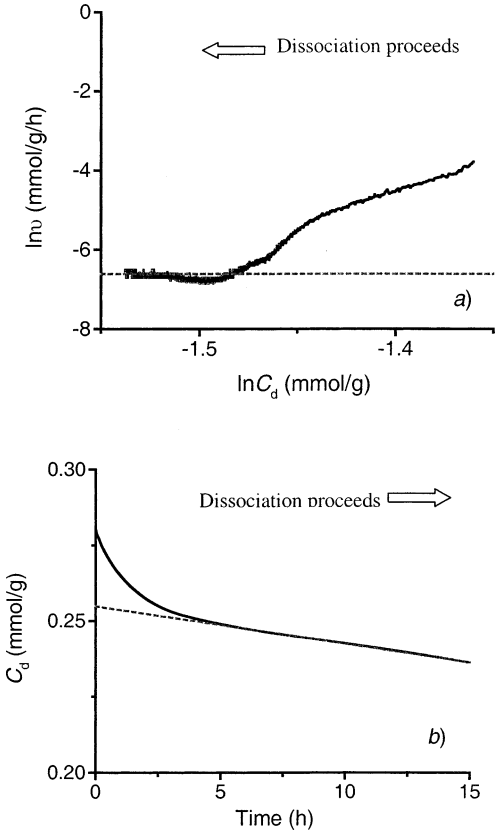

Figure 3. Dissociation kinetics data for the Sil-2N[6]-N_2O_2Na particles in CAPS buffer (pH = 11.0) at 37 °C: (a) ln υ vs ln C_d plot, with a zero slope achieved as dissociation proceeds, and (b) C_d vs t plot, with linearity (zero-order characteristics) achieved after ca. 5 h.

Table 7. "Apparent" Half-Lives ($t_{1/2}$) of Dry Sil-2N[6]-N_2O_2Na Particles at Different Temperatures

	T (°C)		
	−15	23	80
$t_{1/2}$ (min)	1.00×10^5	1.22×10^4	18

Effect of Pendant Amine Structures on the Dissociation Rate. For the Sil-N_2O_2Na particles with different pendant amine structures (see Table 1), chemiluminescence was also used to examine their dissociation kinetics under physiological conditions (PBS, pH 7.4, 37 °C). The results are shown in Table 8. It was found that all of these particles also undergo proton-driven dissociation under physiological conditions, as the chemiluminescence signal is much higher after the PBS buffer is added compared to the NO generated from the dry particles. Linear ln υ−ln C_d plots (data not shown) with a slope greater than 1 were also obtained for all of the fumed silica particles examined. However, their "apparent" half-lives and reaction orders were found to be different than Sil-2N[6]-N_2O_2Na particles, as indicated in Table 8. It has been reported in the literature that the parent amine structure has a significant

(50) Genz, A. K.; Busche, R.; von Engelhardt, W. *Comparative Biochem. Physiol. A−Physiol.* **1997**, *118*, 407.
(51) Gyenge E. L.; Oloman, C. W. *J. Appl. Electrochem.* **2001**, *31*, 243.
(52) Gfatter, R.; Hackl, P.; Braun, F. *Dermatology* **1997**, *195*, 258.

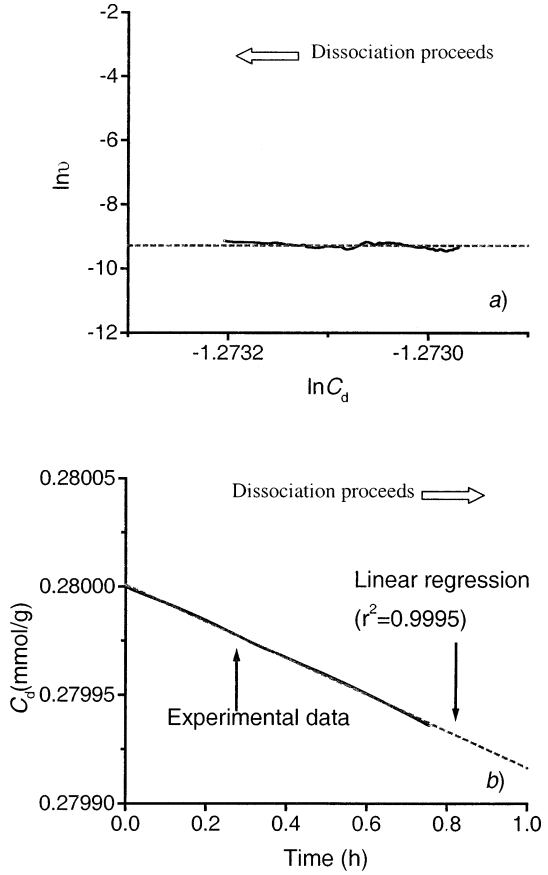

Figure 4. Dissociation kinetics data for the dry Sil-2N[6]-N_2O_2Na particles at −15 °C: (a) ln υ vs ln C_d plot, with a slope of zero, and (b) C_d vs t plot (excellent linearity indicates a zero-order reaction).

Table 8. "Apparent" Half-Lives ($t_{1/2}$) and Reaction Order (n) of Various Sil-N_2O_2Na Particles with Different Parent Amine Structures in PBS (pH 7.4) at 37 °C (2 measurements for each type of particle)

	"apparent" $t_{1/2}$ (min)			n
parent amines	Na^+	K^+	Li^+	Na^+
1N-H	56	53	26	2.45
1N-C1	5.2	6.8	7.2	1.75
2N[2]	144	118	170	1.32
2N[6]	43	40	37	1.69

influence on the rate of *N*-diazeniumdiolate dissociation;[30,31] however, there is still no general rule regarding the correlation between the structure and dissociation rates for the sodium *N*-diazeniumdiolate species. Dissociation kinetics of *N*-diazeniumdiolates is complicated. Indeed, for five solution phase *N*-diazeniumdiolate compounds whose kinetics have been investigated in detail thus far, four different dissociation pathways were identified, even though these compounds all exhibit pseudo-first-order dissociation rates and had similar structures.[30]

Effect of Countercation on the Dissociation Rate. Different alkali metal cations (M = Na^+, K^+, Li^+) do not seem to greatly affect the *N*-diazeniumdiolate dissociation under physiological conditions, as indicated by the almost identical "apparent" half-lives for various Sil-N_2O_2M particles prepared with the different countercations (see Table 8). The apparent half-life of 1N-H Li^+ (i.e., Sil-1N-H-N_2O_2Li), however, appears somewhat shorter than either 1N-H K^+ or 1N-H Na^+, whereas such a difference

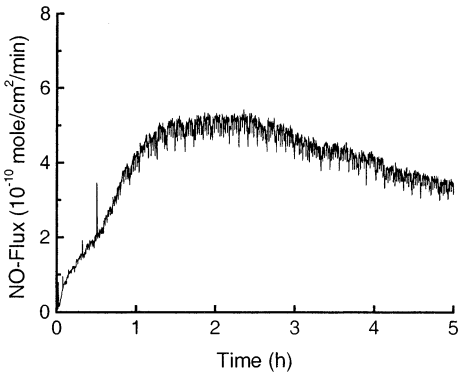

Figure 5. NO-flux profile in PBS (pH 7.4) at 37 °C from a PVC tubing with inner wall coated with PU/Sil-2N[6]-N_2O_2Na material.

is not obviously observed for the secondary amine structures. Apparently, either the extra hydrogen attached to the primary amino nitrogen or the weaker basicity of the primary amine group itself may be responsible for such a difference. Nonetheless, the data shown in Table 8 suggest that the *N*-diazeniumdiolate dissociation rate seems mainly irrelevant to the nature of the countercation. This is consistent with previous results, showing that the nature of the cation does not influence the efficiency of *N*-diazeniumdiolate formation (see Table 5).

In Vivo Blood Compatibility Evaluation of Extracorporeal PVC Tubing Coated with PU/Sil-2N[6]-N_2O_2Na Materials. To examine the potential biomedical application of these new NO-releasing fumed silica particles, polymer matrixes containing the Sil-N_2O_2M materials were formulated to create NO-releasing polymeric films that could be used for coating blood-contacting devices. As an initial model, the Si-2N[6]-N_2O_2Na particles were dispersed at 20 wt % into a polyurethane layer that was coated on the inner wall of biomedical grade Tygon tubing and then used in a rabbit extracorporeal blood circulation system of the type employed previously to evaluate the thromboresistivity of other NO-releasing polymers.[3] Details of the multilayered configuration are described in the Experimental Section. A scanning electron micrograph (SEM) of a cross-section of the final layered structure is shown in Figure 1S, within the Supporting Information file.

The PU/Sil-2N[6]-N_2O_2Na coatings on the inner walls of the Tygon tubings were found to yield NO-flux levels comparable to that from stimulated endothelial cells (4.1×10^{-10} mol/cm^2/min)[26] under physiological conditions throughout 4 h ECC experiments in the rabbit model (see Figure 5). Continuous NO-release from such coatings was observed for at least 4 h, far longer than when the particles are suspended directly in PBS. Further, there was no evidence of any leaching of silica particles from the PU coatings during the experiments (as determined by SEM examination of cross-section images of the tubing wall). After the rabbit experiments, the blood-contacting surfaces of ECC tubings were examined under SEM to access surface thrombosis. As illustrated in Figure 6, fewer thrombi and a significantly lower degree of platelet activation (i.e., irregular platelets with pseudopodia extension instead of round) were observed on the surfaces of NO-releasing ECC circuits compared to control surfaces. Such micrographs were also obtained for four different sections of the tubing used for each experiment, and the effect shown in Figure 6 provides a good picture of the representative average observed for all sections of the tubing

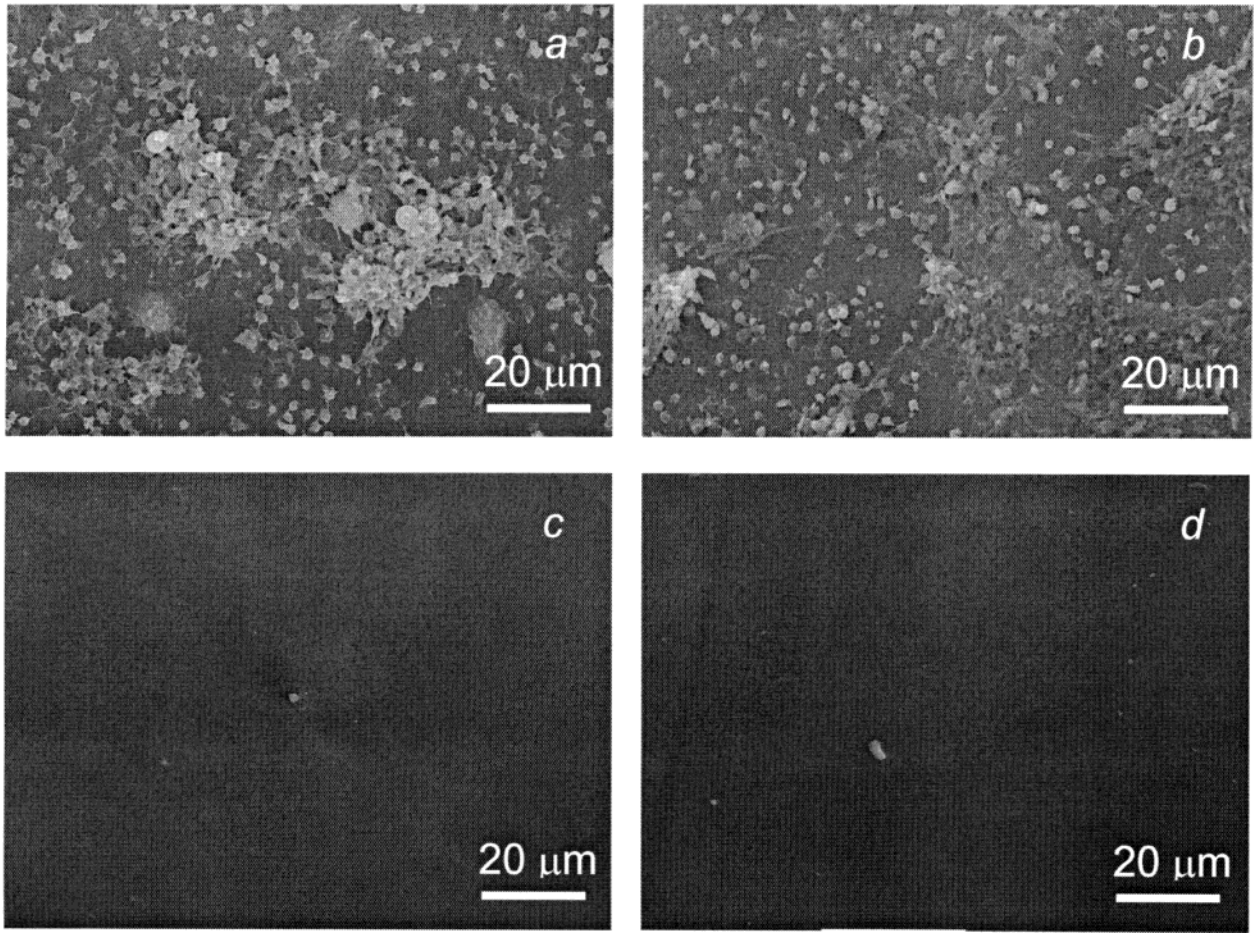

Figure 6. Typical SEM images of different surfaces after 4 h extracorporeal circulation using a rabbit model: (a and b) control coating (PU/silica) surfaces; and (c and d) NO-releasing coating (PU/Sil-2N[6]-N_2O_2Na) surfaces.

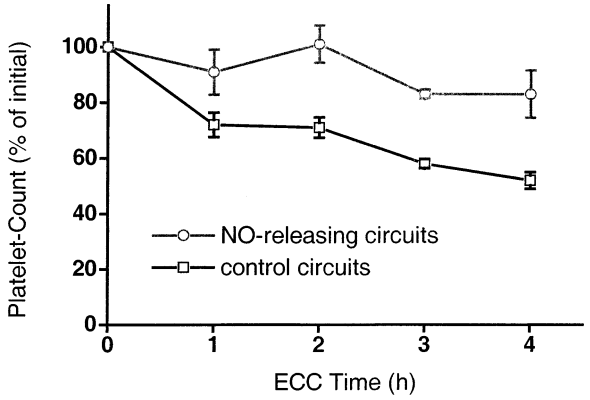

Figure 7. Preliminary platelet maintenance data of NO-releasing circuits (N = 3) and control circuits (N = 3) during ECC experiments.

in all experiments. Further, visual inspections of the circuits following termination of the experiments showed clearly that the control circuits had many more clots on the inner walls than the NO-release circuits. As shown in Figure 7, less platelet consumption was also observed for the NO-releasing ECC circuits (N = 3) compared to control circuits (N = 3). These results demonstrate the improved surface thromboresistivity of the NO-release coating created by embedding the fumed silica particles into a polymeric film. Such results correlate well with previous studies of NO-releasing silicone rubber[11,12] and PVC[3] materials that were evaluated using the same ECC rabbit model.

Conclusions

Nitric oxide-releasing fumed silica particles have been prepared and characterized for the first time. These silica particles can store a relatively large quantity of NO in the form of *N*-diazeniumdiolates, which are stable when kept dry and at low temperature. The NO-release characteristics of the materials are determined by the specific structure of the alkylamines attached to the silica surface. Further, it has been shown that such particles can be blended into a polymer matrix to obtain polymeric films that release NO for extended time periods. Results from this work further demonstrate the potential of the NO-release strategy toward the development of more blood compatible polymers. In addition to preparing more biocompatible medical devices, the use of NO-releasing particles can also be explored in other biomedical/pharmaceutical/cosmetic applications involving other biological functions of NO,[53,54] including vasodilation, antimicrobial,[55] anticancer, neurotransmission, and wound healing.

Acknowledgment. We are grateful for support from the National Institutes of Health through grant NIH EB-00783, and Michigan Critical Care Consultants, Inc.

(53) Snyder, S. H.; Bredt, D. S. *Sci. Am.* **1992** (May), 68.
(54) Feldman, P. L.; Griffith, O. W.; Stuehr, D. J. *Chem. Eng. News* **1993** (Dec 20), 26.
(55) Nablo, B. J.; Chen, T. Y.; Schoenfisch, M. H. *J. Am. Chem. Soc.* **2001**, *123*, 9712.

Supporting Information Available: (I) Summary of calculation methods used to determine degree of surface modification and subsequent efficiency in diazeniumdiolate formation; (II) SEM of tubing; (III) possible reaction schemes for nitrite salt formation. This material is available free of charge via the Internet at http://pubs.acs.org.

JA0291538